

Gross and Fine Structure of Pion Production Excitation Functions in p -Nucleus and Nucleus-Nucleus Reactions

B. Jakobsson,¹ M. Berg,¹ L. Carlén,¹ R. Elmér,¹ A. Fokin,¹ R. Ghetti,¹ J. Mårtensson,¹ B. Norén,¹ A. Oskarsson,¹
H. J. Whitlow,¹ C. Ekström,² G. Ericsson,² J. Romanski,² E. J. van Veldhuizen,² L. Westerberg,² J. Julien,³
Ö. Skeppstedt,⁴ K. Nybö,⁵ T. F. Thorsteinsen,⁵ S. Amirelmi,⁵ M. Guttormsen,⁶ G. Løvholden,⁶ V. Bellini,⁷
F. Palazzolo,⁷ M. L. Sperduto,⁷ J. P. Bondorf,⁸ I. Mishustin,⁸ V. Avdeichikov,⁹ O. V. Lozhkin,¹⁰ and Yu. Murin¹⁰

(CHIC Collaboration)

¹*Department of Physics, University of Lund, Lund, Sweden*

²*The Svedberg Laboratory and Department of Neutron Physics, University of Uppsala, Uppsala, Sweden*

³*Centre d'Etudes Nucléaires, Saclay, France*

⁴*Department of Physics, Chalmers Institute of Technology, Gothenburg, Sweden*

⁵*Department of Physics, University of Bergen, Bergen, Norway*

⁶*Department of Physics, University of Oslo, Oslo, Norway*

⁷*Istituto Nazionale di Fisica Nucleare/Laboratorio Nazionale del Sud, University of Catania, Catania, Italy*

⁸*Niels Bohr Institute, Copenhagen, Denmark*

⁹*Joint Institute for Nuclear Research, Dubna, Russia*

¹⁰*V. G. Khlopin Radium Institute, St. Petersburg, Russia*

(Received 21 October 1996)

Slow ramping of the CELSIUS storage ring has been utilized to measure the yield of charged pions in proton and heavy ion induced collisions with continuously varying beam energy. Boltzmann-Uehling-Uhlenbeck predictions, including Fermi momenta of nucleons in nuclei, follow the general shape of the p -nucleus excitation functions quite well except for a general overestimation of the backward emission. For heavy ion reactions the calculated yield also falls off faster with decreasing beam energy than the data. No statistically significant narrow resonances are observed. [S0031-9007(97)03152-9]

PACS numbers: 25.40.Ve, 24.10.Nz, 25.70.-z

Pions can be produced in hadron-nucleus and nucleus-nucleus collisions, also at energies well below the free nucleon-nucleon (NN) threshold through the collective interaction between several nucleons or through the boost from the internal nucleon momentum. Suggested production mechanisms range from first chance NN scattering [1,2], full cascade prescriptions [3,4], dynamical mean-field + NN collision equations [5–8], predominantly for reactions around and above the NN threshold, to cluster-cluster interactions [9] and fully collective pionic fusion models [10–12], for reactions close to the absolute (collective) threshold. The strong rescattering when pions or deltas propagate through the nuclei must, of course, be introduced in all models.

Many of these models predict the overall features of pion emission well but a detailed selection among them is hampered by the lack of systematic data. By combining slow ramping operation of the CELSIUS storage ring with the range telescope technique, complete excitation functions for π^\pm emission over wide ranges of beam energy can be measured—from the absolute (collective) threshold to well above the (free) NN threshold.

Protons and fully stripped Ne ions were injected into the CELSIUS storage ring [13], accelerated up to the start energy, stored during slow ramping of the magnets with gas-jet target in operation until the final energy was reached, and then finally dumped. The cycle time, 2–5 min, was governed by the requirement that at least $\frac{1}{3}$

of the stored ions should remain. Data were collected continuously during 70–250 s. The start time for slow ramping, the time when the event trigger appeared, and the beam frequency at that time were stored to provide the collision energy. No electron cooling of the beams was introduced. Data from two ramp cycles, one at low energy (169–270 MeV for p and 50A–120A MeV for Ne) and one high energy (250–500 MeV and 100A–400A MeV), were put together. The reproduction of the cycles was very good and data could be added for several hours without increasing the collision energy dispersion (< 0.8 MeV for proton beams and $< 0.9A$ MeV for Ne beams). Gas-jet target thicknesses of between 10^{13} and 10^{14} atoms/cm² for N, Ar, Kr, and Xe gases were employed.

Five 9-element plastic range telescopes were mounted outside thin steel windows in angular positions from 20° to 120° . These telescopes [14] have increasing scintillator thickness to obtain equally broad pion energy bins. The π^+ is identified through pulse shape discrimination technique, utilizing the delayed muon energy signal from the 26 ns, $\pi \rightarrow \mu\nu$ decay [14].

Since the instantaneous luminosity cannot be measured, high energy protons (52–161 MeV) were registered, together with pions, to obtain absolute normalization [last term in Eq. (1)]. Since proton (+ heavy particle) rejection [14] was required in the p -nucleus experiment (99% efficiency), calibration runs were performed with rejected and nonrejected protons registered simultaneously in two

identical telescopes placed at 90° on each side of the beam direction. The total high energy proton yield is translated into absolute cross sections via empirical information [15,16] normalizing standard Boltzmann-Uehling-Uhlenbeck (BUU) [8] or cascade calculations [17] (BUU finally used here). The pion cross section is given by

$$\frac{d\sigma_\pi}{d\Omega} = f_{\text{eff}} \frac{N_\pi}{N_p} \Delta\Omega \left(\frac{N_{\pi nr}^c}{N_{\pi r}^c} \frac{N_{pr}^c}{N_{pnr}^c} \right) \int_{52}^{161} \frac{d^2\sigma_p}{d\Omega dE} dE. \quad (1)$$

The efficiency factor, f_{eff} , contains corrections for decay in flight and during slowdown in detector material, pion scattering in the detector material, and geometry for muon capture [18]. The quantity $\Delta\Omega$ is the relative solid angle correction, c stands for calibration telescope, r for data where proton rejection is used, and nr for data without any rejection. The rejection term, within brackets in Eq. (1), is individually estimated for each stop detector in the calibration runs. The fact that the rejection efficiency for protons is the same in all telescopes within 10% variation was confirmed in a test where both rejected and nonrejected protons were recorded everywhere.

Figure 1 presents examples of differential ($d\sigma/d\Omega$) cross sections of π^+ emitted at 97° in $p + {}^{40}\text{Ar}$ and $p + {}^{\text{nat}}\text{Xe}$ reactions. Figure 1(a) shows the $p + \text{Ar}$ excitation function with 1 MeV beam energy binning. A rather large difference in statistics between the low energy and high energy data sets for $p + \text{Ar}$ introduces the large differences in statistical fluctuations which is not the case for $p + \text{Xe}$ where statistics are comparable between the data sets [Fig. 1(c)]. The normalizing procedure may introduce different systematic errors for the low and high energy data, and therefore we normalize the data sets in the overlapping region to the set with the highest statistics. In no case is there a mismatch between the low energy and high energy data sets exceeding 20%. The complicated normalization procedure is bound to make the errors in the absolute yields larger than in classical fixed target experiments. The error in the absolute yield has contribution from f_{eff} (15%), $\int_{52}^{161} (d^2\sigma_p/d\Omega dE) dE$ (20%), the $r \rightarrow nr$ conversion (12%), the $\Delta\Omega$ determination (4%), the N_π selection efficiency (4%), and the low/high cycle matching (20%). This adds up to a total error of $\sim 35\%$ or slightly more at the lowest beam energies.

The long arrows in Fig. 1 mark the absolute (kinematical) threshold for the reaction, $p + X \rightarrow \pi^+(E_\pi > E_\pi^{\text{min}}, \Theta = 97^\circ) + \dots$, which is calculated from the general threshold condition on the available c.m. energy, $E_{\text{av}} > m_\pi$ where

$$\left(E_{\text{av}} + \sum m_f \right)^2 = (\gamma_A m_A + \gamma_B m_B)^2 - (\vec{\beta}_A \gamma_A m_A + \vec{\beta}_B \gamma_B m_B)^2. \quad (2)$$

m_f denotes here all final (baryonic) fragments. The short arrows denote the experimental cutoff. The background is very small and appears to be flat, which can be ob-

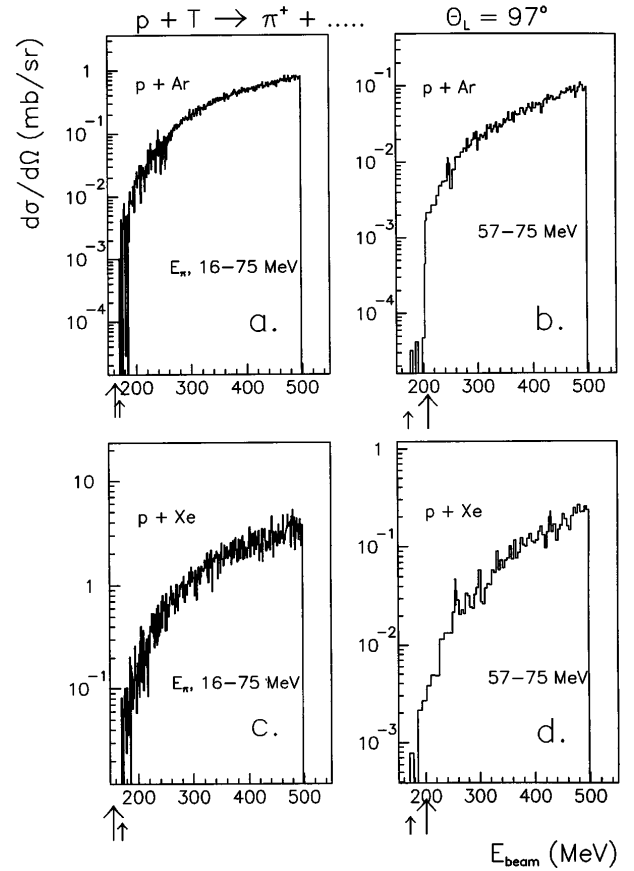


FIG. 1. Differential ($d\sigma/d\Omega$) cross sections of π^+ emitted at 97° in $p + {}^{40}\text{Ar}$ and $p + {}^{\text{nat}}\text{Xe}$ reactions. The beam energy binning is 1 MeV in (a) and (c), 2–4 MeV in (b), and 4–8 MeV in (d). The arrows indicate the absolute threshold and the experimental threshold, as explained in the text. The free $pp \rightarrow \pi^+ \dots$ threshold is ~ 375 MeV in (a) and (c). The typical error bars in (b) and (d) are purely statistical.

served in Figs. 1(b) and 1(d) where the experimental cutoff falls below the absolute threshold of pion production. Figure 1(b) also shows that pions with $E > 57$ MeV are observed even at the lowest possible 1 MeV beam energy bin.

Figure 2 gives differential π^+ cross sections in $p + \text{Ar}$ collisions at three angles and in $\text{Ne} + \text{Ar}$ data at two angles. It should be noticed that the systematic errors in the $\text{Ne} + \text{Ar}$ data are somewhat larger, $\sim 45\%$, than in the $p + \text{Ar}$ data. All data are compared to BUU calculations performed with the code from [8,19].

The numerical BUU implementation is based on the test particle method and uses the parallel ensemble algorithm. 1000 (p) and 500 (Ne) test particles/nucleon have been used. The Fermi momentum of each test particle is given a local value, $P_F = \hbar[\frac{3}{2}\pi^2\rho(r)]^{1/3}$. The initial momentum is chosen either from a sharp sphere homogeneous distribution or from a Gaussian distribution that describes the high momentum components in heavy ion data on particle emission. Nucleons and resonances propagate in a density dependent (Skyrme) mean field [$U(\rho) = A(\rho/\rho_0) + B(\rho/\rho_0)^\sigma$] with a parameter set

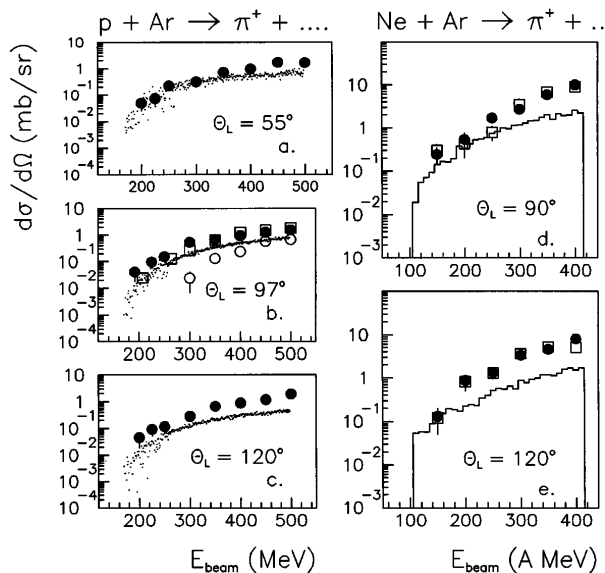


FIG. 2. Differential π^+ cross sections in $p + \text{Ar}$ collisions at three angles (55° , 97° , 120°), and in $\text{Ne} + \text{Ar}$ collisions at two angles (90° , 120°). The points represent BUU calculations where the momenta of the test particles is taken from a Gaussian distribution (filled circles), a homogeneous spherical distribution (open squares), or is neglected (open circles).

typical for a hard, $K = 380$ MeV, equation of state] + Coulomb potential. Pions, produced through Δ and N^* , are treated as free particles interacting with the Coulomb potential only. Reabsorption is taken into account through the process, $N + \pi \rightarrow \Delta$, $\Delta + N \rightarrow N + N$. Resonance production and decay is isotropic and pions as well as nucleons face two-body elastic and inelastic collisions, taking Pauli blocking into account. The calculations proceed for 100 fm/c in 20 (pA) or 10 (AA) impact parameter steps.

The introduction of Fermi motion is necessary in order to reproduce the yields at low beam energies. This is obvious in Fig. 2(b). Generally, the BUU calculations overestimate the π^+ yield, particularly in the backward hemisphere and more for heavy ion collisions than for proton induced collisions. Introducing a momentum dependent local potential should decrease the calculated yield substantially [20,21] and the omission of the s -wave (direct) π production channel may also decrease it somewhat [22]. A shift to a soft equation of state [21] or to a nonisotropic Δ decay distribution will not affect the yield of pions much. Naturally other models should also be confronted with the data, before detailed conclusions can be made.

Figure 3 shows the total yield of π^+ from $p + N$ and $p + \text{Ar}$ collisions. The necessary correction for missing low and high energy pions (5% at low and 50% at high beam energies) is introduced from BUU calculations with a Gaussian internal momentum distribution. This adds another contribution ($\sim 20\%$) to the systematic error which is here increased to $\sim 40\%$.

The experimental ratio between the $p + {}^{14}\text{N}$ and the $p + {}^{40}\text{Ar}$ yield decreases from 2.9 (corresponding to an

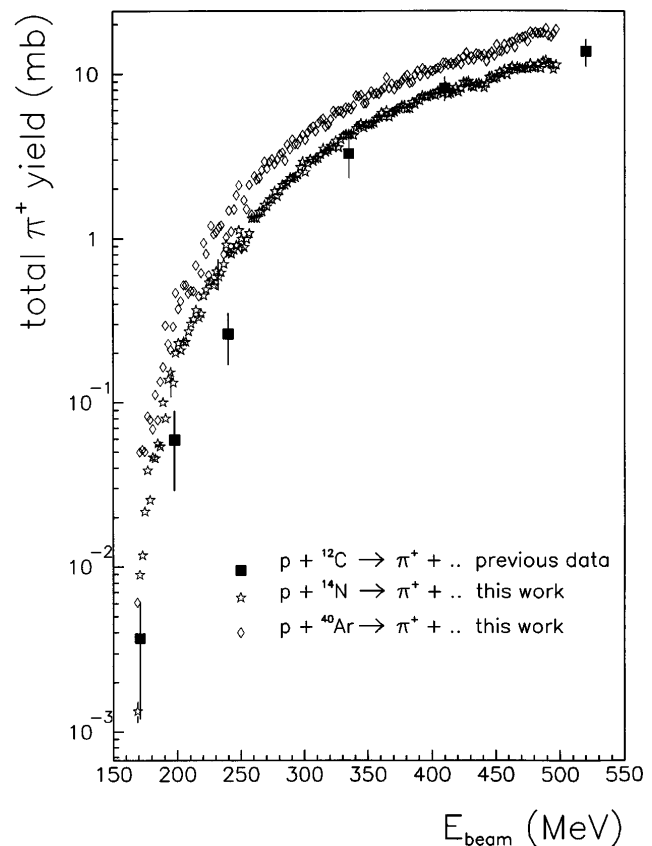


FIG. 3. Energy and angle integrated yield of π^+ from $p + N$ (stars) and $p + \text{Ar}$ (diamonds) collisions. The solid squares are data taken for $p + {}^{12}\text{C}$ reactions [23], in earlier experiments. Note the typical statistical errors in two $p + N$ points.

$A^{1.01}$ dependence) at the lowest energies to 1.5 ($A^{0.40}$) at the highest, indicating a trend to go from a strict volume dependence to nearly a disk dependence, characteristic for peripheral interactions. A comparison to the most systematic data set, reported in the literature for $p + {}^{12}\text{C}$ collisions [23], is made. The agreement between the $p + {}^{12}\text{C}$ data and the $p + N$ data is satisfactory for higher beam energies, but below the free NN threshold (290 MeV) there is up to a factor of 2 difference although an $A^{2/3}$ dependence would predict only a factor of 1.11. The combined statistical (shown in the figure) and systematic errors can explain the difference for each $p + {}^{12}\text{C}$ point except possibly the one at 240 MeV.

Data on yields from a continuously varying beam energy, are ideal in the search for sharp resonances, provided that high enough statistics can be obtained and that both the initial and final states are well enough defined. In this experiment the initial state is well defined with a beam energy dispersion of < 1 MeV, whereas the other two conditions can be questioned. The most intriguing experimental reports on resonances report on π^+ emission at 90° in $p + \text{Cu}$ reactions with a peak at an energy of 350 ± 1 MeV [24–27]. The first explanation, that of dibaryons [24], has later been rejected due to the narrow width of the peak, ~ 1.5 MeV, which does not

agree with the width due to the nucleon Fermi motion in Cu. More recent explanations include two-pion [28] and two- Δ [26] or Δ -ball [29,30] states.

The phenomenon was first observed in the experiments as an enhanced integrated yield of π^+ [24] but later it was stressed that the signal is strongest in the low energy yield, and the low energy to high energy pion ratio was investigated [25,27]. We followed this prescription, and in Fig. 4 we plotted $R = N_{\pi}(16-38 \text{ MeV})/N_{\pi}(38-75 \text{ MeV})$ for π^+ emission at 97° in $p + \text{Ar}$ and $p + \text{Kr}$ reactions. Figures 4(a) and 4(c) show the ratio with 1 MeV beam energy binning, in those regions where statistics allow it ($>250 \text{ MeV}$), whereas a larger bin width (4–12 MeV) is presented in Figs. 4(b) and 4(d). The general trends of decreasing R with increasing beam energy and especially the high value of R at low beam energy in $p + \text{Ar}$ are natural consequences of the kinematics but apart from this, there appears a number of peaks, the most intriguing being the one at 355 MeV in the $p + \text{Kr}$ reaction [Fig. 4(c)]. This is, however, totally washed out in the 4 MeV binning representation [Fig. 4(d)]. The peak point has $R = 0.95 \pm 0.22$, with a “background” level of $R = 0.49 \pm 0.08$. The peak is thus only 2 standard deviations above the normal level while the peak-to-background ratio is 2.1, as compared to the ratio 1.3 reported in [27] for the $N_{\pi}(14.4-32 \text{ MeV})/N_{\pi}(38-80 \text{ MeV})$ ratio in $p + \text{Cu}$. Thus higher statistics is needed to settle this question.

In conclusion, we have demonstrated the power of experiments with slowly ramped beams and gas-jet targets at storage rings. The pion production excitation functions, both in p -nucleus and nucleus-nucleus collisions, agree with the beam energy dependence of the BUU predictions

if (degenerate) Fermi momenta are introduced. The absolute yields are, however, overestimated which possibly can be due to the omission of a momentum dependent interaction potential and/or the s -wave contribution. No statistically significant peaks that indicate narrow resonances are observed, although one candidate— π^+ emission at 97° in $p + \text{Kr}$ reactions at 355 MeV—has been discussed.

The excellent technical support from the TSL accelerator staff is gratefully acknowledged. We thank W. Bauer and B. Li for making their BUU code available to us. We thank the Swedish Natural Science Research Council for its financial support. One of us (V.A.) appreciates the scholarship for the Swedish Institute.

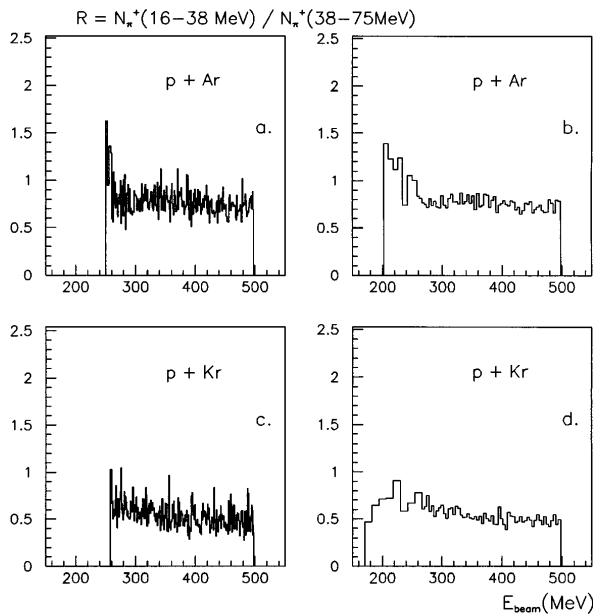


FIG. 4. Ratio between $97^\circ \pi^+$ with a kinetic energy of 16–38 MeV and 38–75 MeV. The beam energy binning is 1 MeV in panels (a) and (c), 4–12 MeV in panels (b) and (d).

- [1] G. F. Bertsch, Phys. Rev. C **15**, 713 (1977).
- [2] B. Jakobsson, J. P. Bondorf, and G. Fai, Phys. Lett. **82B**, 35 (1979).
- [3] K. K. Gudima, H. Iwe, and V. D. Toneev, J. Phys. G **5**, 229 (1978).
- [4] J. Cugnon, T. Mizutani, and J. Vandermeulen, Nucl. Phys. **A532**, 505 (1981).
- [5] W. Cassing, V. Metag, U. Mosel, and K. Niita, Phys. Rep. **188**, 363 (1988).
- [6] P. Schuck *et al.*, Prog. Part. Nucl. Phys. **22**, 181 (1989).
- [7] J. Aichelin, Phys. Rep. **202**, 233 (1991).
- [8] B. Li and W. Bauer, Phys. Rev. C **44**, 450 (1991).
- [9] R. Shyam and J. Knoll, J. Nucl. Phys. A **426**, 606 (1984).
- [10] K. Klingensbeck, K. Dillig, and M. Huber, Phys. Rev. Lett. **47**, 1654 (1981).
- [11] J. Aichelin and G. F. Bertsch, Phys. Lett. **138B**, 350 (1984).
- [12] M. Prakash, P. Braun-Muntzinger, and J. Stachel, Phys. Rev. C **33**, 937 (1986).
- [13] TSL Progress Report 1994–1995, edited by A. Ingemarsson, p. 8.
- [14] B. Norén *et al.*, Nucl. Phys. **A489**, 763 (1988).
- [15] W. A. Richter *et al.*, Phys. Rev. C **49**, 1001 (1994).
- [16] A. A. Cowley *et al.*, Phys. Rev. C **43**, 678 (1991).
- [17] R. E. Prael, Los Alamos Report No. LA-UR-89-3014, 1989.
- [18] G. Sanouillet *et al.*, CEN Saclay Internal Report No. CEA-N-248, 1986.
- [19] B. Li *et al.*, Phys. Rev. C **44**, 2095 (1991).
- [20] J. Aichelin, A. Rosenhauer, G. Peilert, H. Stoecker, and W. Greiner, Phys. Rev. Lett. **58**, 1926 (1987).
- [21] G. Li, D. T. Khoa, T. Maruyama, S. W. Huang, N. Ohtsuka, and A. Faessler, Nucl. Phys. **A534**, 697 (1991).
- [22] Gy. Wolf *et al.*, Nucl. Phys. **A517**, 615 (1990).
- [23] B. Million (private communication); B. Jakobsson, Phys. Scr. **48**, 179 (1993).
- [24] V. A. Krasnov *et al.*, Phys. Lett. **108B**, 11 (1982).
- [25] J. Julien *et al.*, Phys. Lett. **142B**, 340 (1984).
- [26] J. Julien *et al.*, Z. Phys. A **347**, 181 (1994).
- [27] F. Guber *et al.* (to be published).
- [28] P. Schuck, W. Nörenberg, and G. Chanfray, Z. Phys. A **330**, 119 (1988).
- [29] V. A. Khodel, Yad. Fiz. **52**, 1355 (1990) [Sov. J. Nucl. Phys. **52**, 858 (1990)].
- [30] M. Zubkov, Phys. Scr. **48**, 205 (1993).